Physics Letters B 681 (2009) 5–13

Contents lists available at ScienceDirect

Physics Letters B

www.elsevier.com/locate/physletb

Study of the $a_0(980)$ meson via the radiative decay $\phi \to \eta\pi^0\gamma$ with the KLOE detector

KLOE Collaboration

F. Ambrosino [e,f], A. Antonelli [a], M. Antonelli [a], F. Archilli [j,k], C. Bacci [l,m], P. Beltrame [b], G. Bencivenni [a], S. Bertolucci [a], C. Bini [h,i], C. Bloise [a], S. Bocchetta [l,m], F. Bossi [a], P. Branchini [m], P. Campana [a], G. Capon [a], T. Capussela [a], F. Ceradini [l,m], S. Chi [a], G. Chiefari [e,f], P. Ciambrone [a], E. De Lucia [a], A. De Santis [h,i], P. De Simone [a], G. De Zorzi [h,i], A. Denig [b], A. Di Domenico [h,i], C. Di Donato [f], B. Di Micco [l,m], A. Doria [f], M. Dreucci [a], G. Felici [a], A. Ferrari [a], M.L. Ferrer [a], S. Fiore [h,i], C. Forti [a], P. Franzini [h,i], C. Gatti [a], P. Gauzzi [h,i,*], S. Giovannella [a], E. Gorini [c,d], E. Graziani [m], W. Kluge [b], V. Kulikov [p], F. Lacava [h,i], G. Lanfranchi [a], J. Lee-Franzini [a,n], D. Leone [b], M. Martini [a,g], P. Massarotti [e,f], W. Mei [a], S. Meola [e,f], S. Miscetti [a], M. Moulson [a], S. Müller [a], F. Murtas [a], M. Napolitano [e,f], F. Nguyen [l,m], M. Palutan [a], E. Pasqualucci [i], A. Passeri [m], V. Patera [a,g], F. Perfetto [e,f], M. Primavera [d], P. Santangelo [a], G. Saracino [e,f], B. Sciascia [a], A. Sciubba [a,g], A. Sibidanov [a], T. Spadaro [a], M. Testa [h,i], L. Tortora [m], P. Valente [i], G. Venanzoni [a], R. Versaci [a,g], R. Volpe [h,i], G. Xu [a,o]

[a] *Laboratori Nazionali di Frascati dell'INFN, Via E. Fermi 40, I-00044 Frascati, Italy*
[b] *Institut für Experimentelle Kernphysik, Universität Karlsruhe D-76128 Karlsruhe, Germany*
[c] *Dipartimento di Fisica dell'Università del Salento, Via Arnesano, I-73100 Lecce, Italy*
[d] *INFN Sezione di Lecce, Via Arnesano, I-73100 Lecce, Italy*
[e] *Dipartimento di Scienze Fisiche dell'Università "Federico II", Via Cintia, I-80126 Napoli, Italy*
[f] *INFN Sezione di Napoli, Via Cintia, I-80126 Napoli, Italy*
[g] *Dipartimento di Energetica, Sapienza Università di Roma, P.le A. Moro, 2 I-00185 Roma, Italy*
[h] *Dipartimento di Fisica, Sapienza Università di Roma, P.le A. Moro, 2 I-00185 Roma, Italy*
[i] *INFN Sezione di Roma, P.le A. Moro, 2 I-00185 Roma, Italy*
[j] *Dipartimento di Fisica dell'Università di Roma "Tor Vergata", Via della Ricerca Scientifica, 1 I-00133 Roma, Italy*
[k] *INFN Sezione di Roma Tor Vergata, Via della Ricerca Scientifica, 1 I-00133 Roma, Italy*
[l] *Dipartimento di Fisica dell'Università di Roma "Roma Tre", Via della Vasca Navale, 84 I-00146 Roma, Italy*
[m] *INFN Sezione di Roma Tre, Via della Vasca Navale, 84 I-00146 Roma, Italy*
[n] *Physics Department, State University of New York at Stony Brook, Stony Brook, NY 11794-3840, USA*
[o] *Institute of High Energy Physics of Academica Sinica, PO Box 918, Beijing 100049, PR China*
[p] *Institute for Theoretical and Experimental Physics, B. Cheremushkinskaya ul. 25, RU-117218 Moscow, Russia*

ARTICLE INFO

Article history:
Received 16 April 2009
Received in revised form 19 June 2009
Accepted 11 September 2009
Available online 17 September 2009
Editor: M. Doser

PACS:
12.39.Mk
13.20.Jf
13.66.Bc
14.40.Cs

ABSTRACT

We have studied the $\phi \to a_0(980)\gamma$ process with the KLOE detector at the Frascati ϕ-factory DAΦNE by detecting the $\phi \to \eta\pi^0\gamma$ decays in the final states with $\eta \to \gamma\gamma$ and $\eta \to \pi^+\pi^-\pi^0$. We have measured the branching ratios for both final states: $Br(\phi \to \eta\pi^0\gamma) = (7.01 \pm 0.10 \pm 0.20) \times 10^{-5}$ and $(7.12 \pm 0.13 \pm 0.22) \times 10^{-5}$, respectively. We have also extracted the $a_0(980)$ mass and its couplings to $\eta\pi^0$, K^+K^-, and to the ϕ meson from the fit of the $\eta\pi^0$ invariant mass distributions using different phenomenological models.

* Corresponding author at: Dipartimento di Fisica, Sapienza Università di Roma, P.le A. Moro, 2 I-00185 Roma, Italy. Tel.: +390649914266; fax: +39064957697.
E-mail address: paolo.gauzzi@roma1.infn.it (P. Gauzzi).

0370-2693/$ – see front matter © 2009 Elsevier B.V. All rights reserved.
doi:10.1016/j.physletb.2009.09.022

Keywords:
e^+e^- collisions
Scalar mesons
Rare ϕ decays

1. Introduction

The problem of the internal structure of the scalar mesons with mass below 1 GeV is still open [1]. It is controversial whether they are $q\bar{q}$ mesons [2], $qq\bar{q}\bar{q}$ states [3], bound states of a $K\bar{K}$ pair [4] or a mixing of these configurations.

An important part of the program of the KLOE experiment, carried out at the Frascati ϕ-factory DAΦNE, has been dedicated to the study of the radiative decays $\phi(1020) \to P_1 P_2 \gamma$ ($P_{1,2}$ = pseudoscalar mesons). These decays are dominated by the exchange of a scalar meson S in the intermediate state ($\phi \to S\gamma$, and $S \to P_1 P_2$), and both their branching ratios and the $P_1 P_2$ invariant mass shapes depend on the scalar structure.

The $\phi \to \eta\pi^0\gamma$ decay has been already used by KLOE and by other experiments to study the neutral component of the isotriplet $a_0(980)$ [5,6]. This process is well suited to study the $\phi \to a_0(980)\gamma$ dynamics, since it is dominated by the scalar production, with small vector background, contrary to $\pi^0\pi^0\gamma$ and $\pi^+\pi^-\gamma$ cases, where a large irreducible background interferes with the $f_0(980)$ signal [7].

In this Letter the result of the analysis of the $\phi \to \eta\pi^0\gamma$ decay, performed on a sample with 20 times larger statistics than the previously published Letter [5], is presented. The final states corresponding to $\eta \to \gamma\gamma$ and $\eta \to \pi^+\pi^-\pi^0$ have been selected. The $\eta\pi^0$ invariant mass distributions have been fit to two models of parametrization of the $\phi \to a_0(980)\gamma$ decay, to extract the relevant $a_0(980)$ parameters (mass and couplings).

2. DAΦNE and KLOE

The Frascati ϕ-factory DAΦNE is an e^+e^- collider operating at a center of mass energy $\sqrt{s} = M_\phi \simeq 1020$ MeV. The beams collide at an angle of $(\pi - 0.025)$ rad, thus producing ϕ mesons with small momentum ($p_\phi \simeq 13$ MeV) in the horizontal plane. The KLOE detector [8] consists of two main subdetectors: a large volume drift chamber (DC) and a fine sampling lead-scintillating fibers electromagnetic calorimeter (EMC). The whole apparatus is inserted in a 0.52 T axial magnetic field, produced by a superconducting coil. The DC is 3.3 m long, with inner and outer radii of 25 and 200 cm respectively. It contains 12 582 drift cells arranged in 58 stereo layers uniformly distributed in the sensitive volume and it is filled with a gas mixture of 90% helium and 10% isobutane. Its spatial resolution is 200 μm and the tracks coming from the beam interaction point (IP) are reconstructed with $\sigma(p_\perp)/p_\perp \leqslant 0.4\%$. The position resolution for two track vertices is about 3 mm.

The DC is surrounded by the EMC, that covers 98% of the solid angle, and is divided into a barrel, made of 24 trapezoidal modules about 4 m long, with the fibres running parallel to the barrel axis, and two endcaps of 32 module each, with fibers aligned vertically. The read-out granularity is $\sim 4.4 \times 4.4$ cm^2, for a total of 2440 cells, read at both ends by photomultipliers. The coordinate of a particle along the fiber direction is reconstructed from the difference of the arrival time of the signals at the two ends of the cell. Cells close in time and space are grouped together into clusters. The cluster energy is the sum of the cell energies, while the cluster time and position are energy weighed averages. The energy and time resolutions for photons are $\sigma_E/E = 5.7\%/\sqrt{E(\text{GeV})}$ and $\sigma_t = 57$ ps$/\sqrt{E(\text{GeV})} \oplus 100$ ps, respectively. Cluster positions are measured with resolutions of 1.3 cm in the coordinates transverse to the fibers, and 1.2 cm$/\sqrt{E(\text{GeV})}$ in the longitudinal coordinate. The detection efficiency for photons of $E \simeq 20$ MeV is greater than 80% and reaches almost 100% at $E > 80$ MeV.

The KLOE trigger is based on the detection of two energy deposits in the EMC, with $E > 50$ MeV in the barrel and $E > 150$ MeV in the endcaps.

3. Event selection

The results are based on the data collected during the 2001–2002 run, at $\sqrt{s} \simeq M_\phi$. Of the two selected decay chains, the fully neutral one is characterized by high statistics and large background, while the charged one has small background but lower statistics. These two decay chains have been selected with different criteria and slightly different data samples have been used: 414 pb^{-1} for the fully neutral and 383 pb^{-1} for the charged decay. Monte Carlo (MC) samples of signal and of background processes have been produced with the simulation program of the experiment [9]. They have been generated on a run-by-run basis, simulating the machine operating conditions and background levels as measured in the data. Three MC samples, generated with different luminosity scale factors ($\text{LSF} = L_{\text{MC}}/L_{\text{data}}$), have been used:

1. The *rad* sample contains all the radiative ϕ-decays plus the non-resonant process $e^+e^- \to \omega\pi^0$, with LSF = 5;
2. The *kk* sample contains $\phi \to K^0\overline{K^0}$ with all subsequent kaon decays generated with LSF = 1;
3. The *all* sample contains all the ϕ decays with LSF = 1/5; it is used to find possible backgrounds not included in the two main samples.

The shape of the $\eta\pi^0$ invariant mass distribution has been simulated according to the spectrum obtained from the previously published analysis [5].

3.1. $\phi \to \eta\pi^0\gamma$ with $\eta \to \gamma\gamma$

This final state is characterized by five prompt photons originating from the IP. A prompt photon is defined as an EMC cluster not associated to any charged track in the DC and satisfying the condition $|t - r/c| < \min[5\sigma_t(E), 2\text{ ns}]$, where t is the photon flight time, r is the corresponding path length, and c is the speed of light. Events with exactly five prompt clusters, with $E > 3$ MeV and polar angle $\vartheta > 21°$ with respect to the beam line, are selected.

The main background originates from the other five photon final states, $\phi \to f_0(980)\gamma \to \pi^0\pi^0\gamma$ and $e^+e^- \to \omega\pi^0 \to \pi^0\pi^0\gamma$, and from the seven photon process, $\phi \to \eta\gamma$ with $\eta \to 3\pi^0$, which can mimic five photon events due to either photon loss or cluster merging. Also the three photon final states, $\phi \to \eta(\pi^0)\gamma$ with $\eta(\pi^0) \to \gamma\gamma$, give a small contribution to the selected sample, when fake clusters are produced either by accidental coincidence with machine background or by cluster splittings. Other background processes are negligible.

The following analysis steps are then applied to the selected events.

1. First kinematic fit which imposes the total 4-momentum conservation and the speed of light for each photon, with 9 degrees of freedom. Events with $\chi^2_{\text{fit1}} > 27$ are rejected. A cut

Table 1
Background processes for $\phi \to \eta\pi^0\gamma$, with $\eta \to \gamma\gamma$. (S/B)$_1$ is the signal to background ratio after the preselection, (S/B)$_2$ the same ratio at the end of the whole analysis chain. The reweighing factors, w, are also listed. Last column reports the final background estimate.

	Process	(S/B)$_1$	(S/B)$_2$	w	Background events
1	$\phi \to f_0\gamma \to \pi^0\pi^0\gamma$	0.40	4.4	1.24 ± 0.02	5062 ± 60
2	$e^+e^- \to \omega\pi^0 \to \pi^0\pi^0\gamma$	0.14	3.1	0.96 ± 0.01	3825 ± 37
3	$\phi \to \eta\gamma$ with $\eta \to 3\pi^0$	0.10	2.8	1.12 ± 0.04	7248 ± 78
4	$\phi \to \eta\gamma$ with $\eta \to \gamma\gamma$	1.6	200	2.89 ± 0.13	197 ± 11
5	$\phi \to \pi^0\gamma$	10	–	–	–
Total background		0.05	1.0		$16\,332 \pm 86$

at 980 MeV on the total energy of the three most energetic photons is also applied to reject residual three photon events (processes 4 and 5 of Table 1).

2. Search for the best photon pairing to η's and π^0's, by choosing the combination that minimizes the χ^2-like variable ($i, j, k, l = 1, \ldots, 5$ are the photon indices):

$$\chi^2_{\text{pair}} = \frac{(M_{ij} - M_{P_1})^2}{\sigma^2_{M_{P_1}}} + \frac{(M_{kl} - M_{P_2})^2}{\sigma^2_{M_{P_2}}}$$

for both $P_1P_2 = \eta\pi^0$ (signal) or $\pi^0\pi^0$ (background) hypotheses. $\sigma_{M_{\pi^0}}$ and σ_{M_η} are the width of the π^0 and η peaks after the first kinematic fit ($\sigma_{M_{\pi^0}} = 6$ MeV and $\sigma_{M_\eta} = 9$ MeV).

3. Second kinematic fit with the two additional constraints of the masses of the intermediate particles. The number of degrees of freedom is 11.

Background from process 1 and 3 of Table 1 dominates the tail of the distribution of the χ^2_{fit2} of the second kinematic fit, as shown in Fig. 1, and it can be reduced by cutting at $\chi^2_{\text{fit2}} < 24$. By using the photon pairing in the background hypothesis, $\pi^0\pi^0\gamma$, the Dalitz plot of Fig. 1 is obtained: the $f_0\gamma$ background populates the lower right corner, while the two straight bands are the contribution of $\omega\pi^0$. The a_0 signal is contained in the region between these bands. The $\omega\pi^0$ background is strongly reduced by cutting out the two bands shown in Fig. 1.

Assuming the background hypothesis $\omega\pi^0$, the angle $\theta^\star$ between the non associated photon and the ω flight direction can be defined. The regions at large $|\cos\theta^\star|$ (Fig. 2(left)) are dominated by $\omega\pi^0$ and $f_0\gamma$ backgrounds. The cut $|\cos\theta^\star| < 0.8$ is then applied. Another effective cut to reduce the $f_0\gamma$ background is $\theta_{23} > 42°$ (Fig. 2(right)), where θ_{23} is the angle between the second and third photons ordered by decreasing energy.

After these cuts the overall selection efficiency, evaluated by MC, is almost independent from the $\eta\pi^0$ invariant mass and its average value is 38.5%. The final sample consists of 29 601 events and the expected S/B ratio is about 1.0 (see Table 1). The residual background is irreducible and has to be evaluated and subtracted. In order to obtain a precise evaluation of the amount of each background process, the following procedure has been adopted.

1. A data control sample dominated by each specific background process, with a signal content below few percent, has been selected.
2. Selected kinematical distributions have been fit to the corresponding MC shapes.
3. The ratio of the number of events found by the fit and the number of expected events from MC is the weight assigned to that process (see Table 1). This weight is a correction factor for the absolute value of the MC cross section for that specific background.

Since these correction factors are correlated, a combined fit on the four data samples, with all the weights as free parameters, has been performed. The results are in agreement with the values obtained from the separate fits, and the correlation matrix is shown in Table 2. In last column of Table 1 the applied weights and the numbers of background events in the final sample are listed. The uncertainties are the combination of MC statistics and of the systematics on the applied weights. The correlations have also been taken into account. After the background subtraction the number of signal event is $13\,269 \pm 192$. In Fig. 3 the $\eta\pi^0$ invariant mass distribution of the final sample is shown together with the background contributions. The invariant mass resolution is about 4 MeV, with non-gaussian tails mainly due to wrong photon combinations. In the same figure, the distribution of the polar angle θ_{rec} of the recoil photon is plotted. After the background subtraction good agreement with the expected $1 + \cos^2\theta_{\text{rec}}$ behaviour is obtained.

Table 2
Correlation coefficients among the MC correction factors.

	$w_{f_0\gamma}$	$w_{\omega\pi^0}$	$w_{\eta\gamma7}$	$w_{\eta\gamma3}$
$w_{f_0\gamma}$	1.			
$w_{\omega\pi^0}$	−0.057	1.		
$w_{\eta\gamma7}$	−0.358	−0.329	1.	
$w_{\eta\gamma3}$	0.053	−0.025	−0.028	1.

3.2. $\phi \to \eta\pi^0\gamma$ with $\eta \to \pi^+\pi^-\pi^0$

With respect to the fully neutral one, this decay provides a lower statistics since the branching ratio of $\eta \to \pi^+\pi^-\pi^0$ is smaller than for $\eta \to \gamma\gamma$. Moreover a lower acceptance is expected due to the larger number of particles to be detected. However in this case there is a smaller background contamination, since no other final state with two tracks and five photons has a significant branching ratio from the ϕ. The main sources of background are due to final states with two tracks and either four or six photons. In order of importance there are: $e^+e^- \to \omega\pi^0$ with $\omega \to \pi^+\pi^-\pi^0$ and a fake cluster; $\phi \to K_SK_L$ with $K_S \to \pi^+\pi^-$ and prompt $K_L \to 3\pi^0$ with one photon lost; $\phi \to K_SK_L$ with $K_S \to \pi^0\pi^0$ and prompt $K_L \to \pi^+\pi^-\pi^0$ or $\pi\ell\nu$ with either one photon lost or one fake cluster; $\phi \to \eta\gamma$ with $\eta \to \pi^+\pi^-\pi^0$ plus two fake clusters.

The signal preselection requires the detection of two charged tracks and of five photons. The following requirements are then applied:

1. A vertex with two opposite sign tracks in a cylinder, around the IP, of 5 cm radius and 11 cm length;
2. Five prompt photons with $E > 10$ MeV;
3. Total energy in the range $900 < E_{\text{tot}} < 1160$ MeV and total momentum $|\vec{P}_{\text{tot}}| < 110$ MeV/c;
4. The scalar sum of the momenta of the two pions $P_\Sigma = |\vec{p}_1| + |\vec{p}_2|$, outside the range $418 < P_\Sigma < 430$ MeV/c, which identifies events with $K_S \to \pi^+\pi^-$.

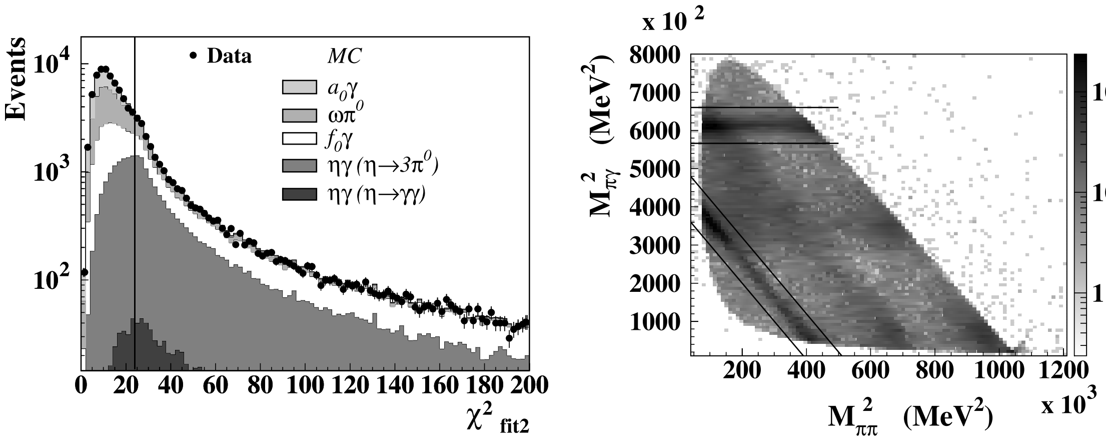

Fig. 1. Right: χ^2 of the second kinematic fit; the applied cut at $\chi^2_{\mathrm{fit2}} = 24$ is also shown. Left: Dalitz plot of data in the background hypothesis ($\pi^0\pi^0\gamma$).

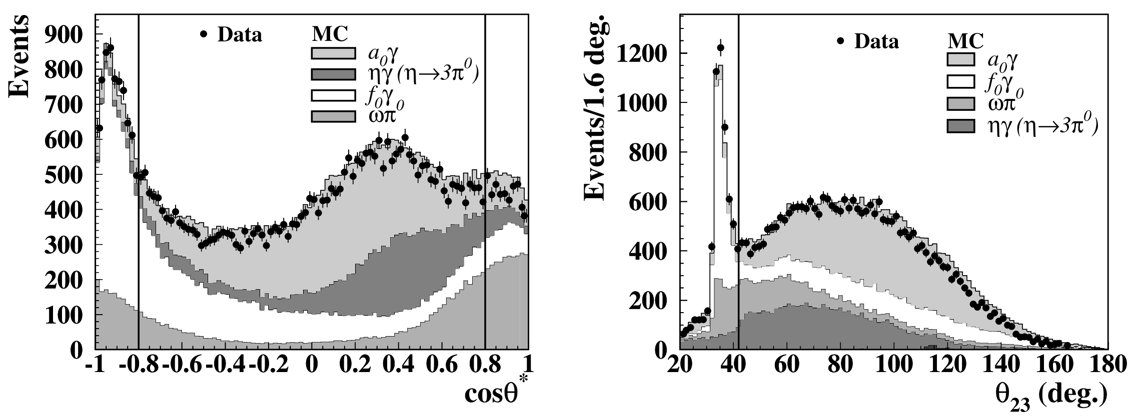

Fig. 2. Left: $\cos\theta^\star$ distribution (see text for explanation). Right: angle between the second and third photons ordered by decreasing energy (vertical lines represent the applied cuts).

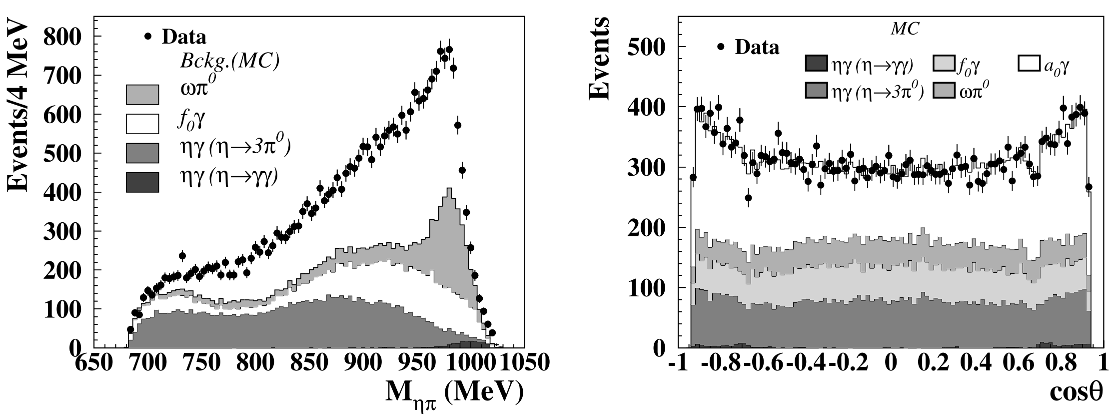

Fig. 3. Left: $\eta\pi^0$ invariant mass distribution of the neutral channel. Right: distribution of the cosine of the polar angle of the recoil photon (dots), compared with the MC expectation (solid line).

Events surviving this preselection go to the kinematic fit stage, similar to that of the neutral channel.

1. A kinematic fit with 9 degrees of freedom is performed by imposing only the total 4-momentum conservation and speed of light for the photons; events with $\chi^2_{\mathrm{fit1}} < 17$ are retained.
2. Photons are combined to build π^0's and η's. There are 15 possibilities to get two π^0's out of five photons. For each of them there are two choices in the association of one π^0 to the $\pi^+\pi^-$ pair. For each of these 30 combinations χ^2_{pair} is computed according to ($i, j, k, l = 1, \ldots, 5$ are the photon indices):

$$\chi^2_{\mathrm{pair}} = \frac{(M_{ij} - M_{\pi^0})^2}{\sigma^2_{M_{\pi^0}}} + \frac{(M_{kl} - M_{\pi^0})^2}{\sigma^2_{M_{\pi^0}}} + \frac{(M_{\pi^+\pi^-\pi^0} - M_\eta)^2}{\sigma^2_{M_\eta}}.$$

   Events with at least one combination with $\chi^2_{\mathrm{pair}} < 10$ are retained.
3. The second kinematic fit is performed on all the combinations selected by the previous step adding the three mass constraints, for a total of 12 degrees of freedom. The combination

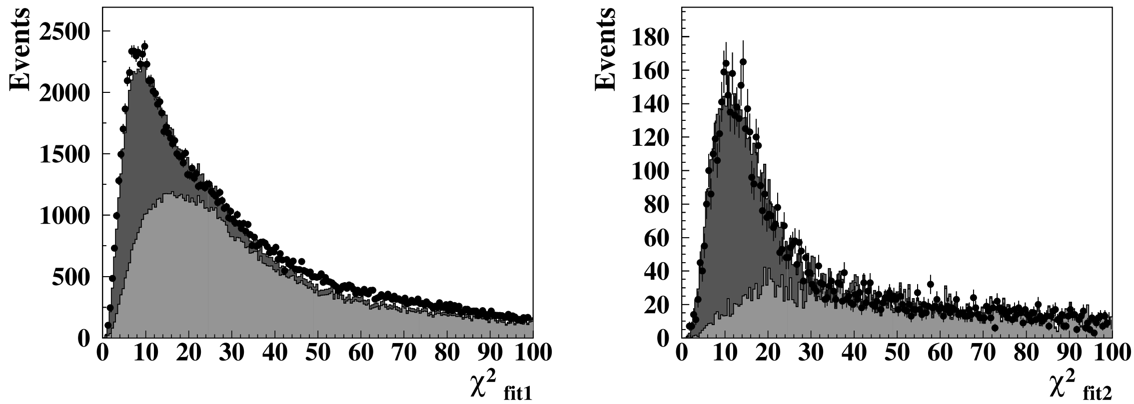

Fig. 4. χ^2 distributions for the first (left) and second (right) kinematic fit. The selected data sample (points) is compared to the MC expectation (dark grey histograms) given by the weighed sum of the signal and the estimated background (light grey histograms).

with the lowest χ^2_{fit2} is chosen. Only events with $\chi^2_{fit2} < 20$ are retained.

4. Finally, events with the recoil photon energy below 20 MeV are discarded to remove events with a spurious low energy photon.

The final sample consists of 4181 events. The overall selection efficiency for the signal, evaluated by MC, is 19.4%, almost independent from the $\eta\pi^0$ invariant mass, decreasing only at very high invariant mass values. Fig. 4 shows the data–MC agreement for the χ^2 distributions of the first and second kinematic fits. The MC distributions include signal and background events. The mass resolution is about 4 MeV for all mass values, with non-gaussian tails, mainly due to events with a wrong photon combination.

The residual background is evaluated by applying the selection procedure on MC samples and by checking the absolute normalization on background enriched data control samples. In order to properly normalize the observed numbers of events, data and MC samples after the preselection but before the kinematic fit have been used. At this level the expected contribution of the signal does not exceed 2–3%. Four variables have been chosen to compare data and MC samples: E_{tot}, $|\vec{P}_{tot}|$, $M_{\gamma\gamma}$ and $M_{\pi\pi\gamma\gamma}$ where $M_{\gamma\gamma}$ is the invariant mass of any pair of photons (10 combinations per event) and $M_{\pi\pi\gamma\gamma}$ is the invariant mass of the two pions and any pair of two photons (again 10 combinations per event). The four distributions for the data are simultaneously fit with the weighed sum of the same MC distributions for each background sample and for the signal. The weights of the *rad* and *kk* samples are the free parameters. $w_{rad} = 0.45$ and $w_{kk} = 1.3$ are obtained, from which the numbers of background events $B_{rad} = 307$ and $B_{kk} = 264$ are estimated. 8 additional background events from the *all* sample have also to be taken into account. The fit has been repeated separately on each control distribution and the spread obtained in the estimated number of events is taken as systematic uncertainty. The total number of background events is 579 ± 27, where the uncertainty is the quadratic sum of the statistical and the systematic uncertainties. This background accounts for about 14% of the selected events.

Fig. 5 shows the $\eta\pi^0$ invariant mass distribution. In the same figure, the distribution of the polar angle of the recoil photon is shown, and is compared to the MC expected behaviour. Also in this case the distribution agrees with the $1 + \cos^2\theta_{rec}$ dependence of the signal.

3.3. Branching ratio evaluation

The branching ratio of the process $\phi \to \eta\pi^0\gamma$ is obtained from the formula

Table 3
Main sources of systematic uncertainty on the branching ratio (3).

Source	Uncertainty ($\times 10^{-5}$)
Photon counting	0.08
Selection efficiency	0.12
$Br(\eta \to \gamma\gamma)$	0.04
$Br(\phi \to \eta\gamma)$	0.13
$Br(\eta \to \pi^0\pi^0\pi^0)$	0.05

$$Br(\phi \to \eta\pi^0\gamma) = \frac{N_f - B_f}{\varepsilon_f N_\phi^{(f)} Br(\eta \to f)} \quad (f = \gamma\gamma, \pi^+\pi^-\pi^0) \quad (1)$$

where N_f is the total number of selected events, B_f the estimated background, ε_f is the average efficiency. N_ϕ is the number of produced ϕ mesons evaluated from the number $N_{\eta\gamma}$ of $\phi \to \eta\gamma$ with $\eta \to \pi^0\pi^0\pi^0$ events,

$$N_\phi = \frac{N_{\eta\gamma}}{\varepsilon_{\eta\gamma} Br(\phi \to \eta\gamma) Br(\eta \to \pi^0\pi^0\pi^0)}. \quad (2)$$

The $Br(\pi^0 \to \gamma\gamma)$ is not included in Eqs. (1) and (2) since it has been already taken into account in the MC. The normalization sample has been selected by requiring no tracks in the DC and six or more prompt clusters in the EMC, in the same runs used for the signal selection. $N_{\eta\gamma} = 4.2 \times 10^6$ events have been found in the sample used for the analysis of the fully neutral decay chain, with efficiency $\varepsilon_{\eta\gamma} = 81\%$, corresponding to $N_\phi^{(\gamma\gamma)} = (1.24 \pm 0.03) \times 10^9$.

By using $Br(\eta \to \gamma\gamma) = (39.31 \pm 0.20)\%$ [10], the branching ratio is obtained:

$$Br(\phi \to \eta\pi^0\gamma) = (7.01 \pm 0.10 \pm 0.20) \times 10^{-5}. \quad (3)$$

The first uncertainty is due to statistics and to the background subtraction. Several sources of systematics have been taken into account (see Table 3): photon counting (dominated by the detection efficiency for low energy photons), the data–MC discrepancies in the evaluation of the selection efficiency, and the normalization uncertainty.

The data sample analyzed for the charged decay channel is slightly smaller than the other one, $N_\phi^{(\pi^+\pi^-\pi^0)} = (1.15 \pm 0.03) \times 10^9$. By using $Br(\eta \to \pi^+\pi^-\pi^0) = (22.73 \pm 0.28)\%$ [10]

$$Br(\phi \to \eta\pi^0\gamma) = (7.12 \pm 0.13 \pm 0.22) \times 10^{-5} \quad (4)$$

is obtained. The first uncertainty is the quadratic sum of the statistical uncertainty on $N_{\pi^+\pi^-\pi^0}$ and of the uncertainty on the background; the second one is systematic, mainly due to the absolute normalization, and includes a 1% error due to the efficiency evaluation.

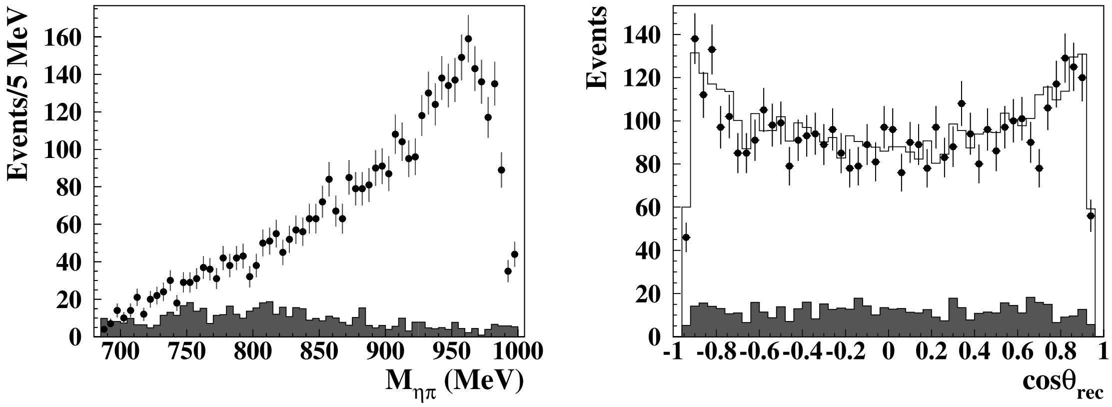

Fig. 5. Left: $\eta\pi^0$ invariant mass distribution for the final data sample (points) compared to the estimated background (dark histogram). Right: polar angle of the recoil photon for data (points) and for MC expectations (histogram). Dark histogram represents the background.

The two branching ratios (3) and (4) are compatible with the old KLOE results: $(8.51 \pm 0.51 \pm 0.57) \times 10^{-5} (\eta \to \gamma\gamma)$ and $(7.96 \pm 0.60 \pm 0.40) \times 10^{-5} (\eta \to \pi^+\pi^-\pi^0)$ [5]. By combining the two results, taking into account the common normalization error

$$Br(\phi \to \eta\pi^0\gamma) = (7.06 \pm 0.22) \times 10^{-5} \quad (5)$$

is obtained, where the uncertainty is both statistic and systematic.

4. Fit of the $\eta\pi^0$ invariant mass distributions

In order to extract the relevant parameters of the a_0, a simultaneous fit, with the same set of free parameters, has been performed on the two $\eta\pi^0$ invariant mass distributions, by minimizing the following χ^2:

$$\chi^2 = \sum_{f=\gamma\gamma,\pi^+\pi^-\pi^0} \sum_{i=1}^{n_f} \frac{(N_i^{(f)} - B_i^{(f)} - E_i^{(f)})^2}{\sigma_i^{(f)2}}$$

where n_f is the number of bins of respectively the fully neutral and charged $\eta\pi^0$ mass distribution; N_i is the content of the i-th bin and B_i is the number of background events to be subtracted from the i-th bin. The expected number of events, E_i, can be written as

$$E_i^{(f)} = N_\phi^{(f)} \sum_{j=1}^{n_f} \varepsilon_{ij}^{(f)} \frac{1}{\Gamma_\phi} \int_{\mathrm{bin}\,j} \frac{d\Gamma_{th}(\phi \to \eta\pi^0\gamma)}{dm} dm \times Br(\eta \to f)$$

where $m = M_{\eta\pi^0}$, and $\Gamma_\phi = 4.26$ MeV [10]. $\varepsilon_{ij}^{(f)}$ is the efficiency matrix (also referred to as smearing matrix), representing the probability of a signal event with "true" mass in the j-th bin of the spectrum to be reconstructed in the i-th bin. The efficiency matrices, evaluated by MC, are almost diagonal; the off-diagonal elements take into account resolution effects as well as wrong photon pairings. The differential decay width $d\Gamma_{th}/dm$ has been parametrized according to two different models.

In the "Kaon Loop" (KL) model [11] the ϕ is coupled to the scalar meson through a loop of charged kaons. The theoretical function can be written as

$$\frac{d\Gamma_{th}(\phi \to \eta\pi^0\gamma)}{dm} = \frac{d\Gamma_{\mathrm{scal}}}{dm} + \frac{d\Gamma_{\mathrm{vect}}}{dm} + \frac{d\Gamma_{\mathrm{interf}}}{dm}. \quad (6)$$

The scalar term $d\Gamma_{\mathrm{scal}}/dm$ is described in some details in Appendix A. $d\Gamma_{\mathrm{vect}}/dm$, is dominated by $\phi \to \rho\pi^0$ with $\rho \to \eta\gamma$ and is described in the framework of the Vector Dominance Models (VDM) [12]. Last term is the interference between the scalar and the vector amplitudes.

The free fit parameters are: the a_0 mass, the couplings $g_{a_0K^+K^-}$, $g_{a_0\eta\pi^0}$, the branching ratio of the vector contribution, the relative phase δ between scalar and vector amplitudes, and, as a relative normalization between the two different final states, the ratio $R_\eta = Br(\eta \to \gamma\gamma)/Br(\eta \to \pi^+\pi^-\pi^0)$.

An alternative parametrization of the amplitude of the decay $\phi \to \eta\pi^0\gamma$ has been also used, following Ref. [13]. A point-like coupling of the scalar to the ϕ meson is assumed, hence this model will be called "No Structure" (NS) in the following. The scalar meson is parametrized as a Breit–Wigner interfering with a polynomial scalar background and with a vector background (see Appendix B). The free parameters in this case are the couplings $g_{a_0K^+K^-}$, $g_{a_0\eta\pi^0}$, and $g_{\phi a_0\gamma}$, the ratio R_η, the branching ratio of the vector background, and two complex coefficients, b_0 and b_1, of the scalar background. The a_0 mass is fixed to avoid fit instabilities, due the large number of free parameters, and due to the large cancellations that occur among the terms of Eq. (9). The chosen value of the a_0 mass is the result of the KL fit.

The fit results are shown in Fig. 6, and the parameter values are listed in Table 4. Good χ^2 probability is obtained for both models.

The ratio R_η is in good agreement with the PDG value 1.729 ± 0.028 [10], confirming that the two samples are consistent with each other.

A vector background smaller than the VDM predictions, $(3\text{–}5) \times 10^{-6}$ [12,15], is found in both fits, indicating that the $\phi \to \eta\pi^0\gamma$ process is largely dominated by $\phi \to a_0\gamma$.

In the KL case, the a_0 mass is in agreement with the PDG value (985.1 ± 1.3) MeV [10]. A ratio of the squared coupling constants $R_{a_0} = g^2_{a_0K^+K^-}/g^2_{a_0\eta\pi^0} = 0.58 \pm 0.03 \pm 0.03$ can be derived in the KL case. The couplings $g_{a_0K^+K^-}$ and $g_{a_0\eta\pi^0}$ of the NS fit and therefore the ratio $R_{a_0} = 0.67 \pm 0.04 \pm 0.13$ are in agreement with the KL values.

This ratio R_{a_0} is in good agreement with the previous measurements: the SND Collaboration obtained $R_{a_0} = 1.8^{+2.5}_{-1.5}$ [6] using $\phi \to \eta\pi^0\gamma \to 5\gamma$ with low statistics, while a more precise determination has been obtained with the Crystal Barrel data on $\bar{p}p$ annihilation at rest into $\omega\eta\pi^0$ and $\eta\pi^0\pi^0$, $R_{a_0} = 0.58 \pm 0.09$ [16]. A recent reanalysis of those data gave $R_{a_0} = 0.525 \pm 0.035 \pm 0.025$ [17].[1]

The $g_{\phi a_0\gamma}$ is not a free parameter of KL model, but can be obtained according to the formula:

[1] The authors of Refs. [16] and [17] define $g^2_{a_0KK} = 2g^2_{a_0K^+K^-}$, therefore their ratio $g^2_{a_0KK}/g^2_{a_0\eta\pi^0}$ is twice the ratio R_{a_0} used in this Letter.

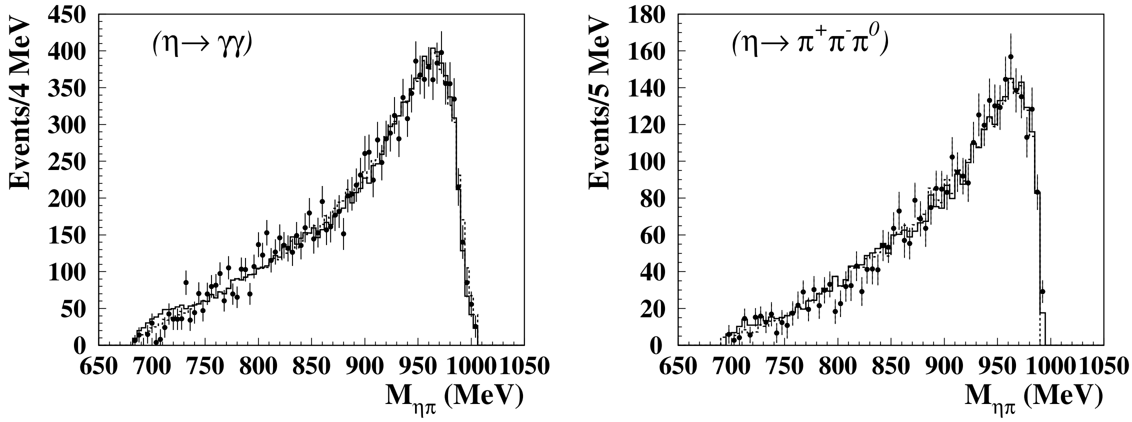

Fig. 6. Fit results: points are data after background subtraction; histograms represent the fit functions for KL (solid) and NS (dashed) models.

Table 4
Fit results for KL and NS models.

	KL	NS
M_{a_0} (MeV)	$982.5 \pm 1.6 \pm 1.1$	982.5 (fixed)
$g_{a_0K^+K^-}$ (GeV)	$2.15 \pm 0.06 \pm 0.06$	$2.01 \pm 0.07 \pm 0.28$
$g_{a_0\eta\pi^0}$ (GeV)	$2.82 \pm 0.03 \pm 0.04$	$2.46 \pm 0.08 \pm 0.11$
$g_{\phi a_0\gamma}$ (GeV^{-1})		$1.83 \pm 0.03 \pm 0.08$
δ (deg.)	$222 \pm 13 \pm 3$	
B.r. of vector background($\times 10^6$)	$0.92 \pm 0.40 \pm 0.15$	~ 0
R_η	$1.70 \pm 0.04 \pm 0.03$	$1.70 \pm 0.03 \pm 0.01$
$\lvert b_0 \rvert$		$14.9 \pm 0.6 \pm 0.5$
arg(b_0) (deg.)		$38.3 \pm 1.1 \pm 0.6$
$\lvert b_1 \rvert$		$21.3 \pm 1.4 \pm 0.9$
arg(b_1) (deg.)		$57.3 \pm 1.4 \pm 1.1$
χ^2/ndf	157.1/136	140.6/133
$P(\chi^2)$	10.4%	30.9%

Table 5
Correlation coefficients among the relevant a_0 parameters.

	KL model				NS model		
	M_{a_0}	$g_{a_0K^+K^-}$	$g_{a_0\eta\pi^0}$		$g_{a_0K^+K^-}$	$g_{a_0\eta\pi^0}$	$g_{\phi a_0\gamma}$
M_{a_0}	1.			$g_{a_0K^+K^-}$	1.		
$g_{a_0K^+K^-}$	0.931	1.		$g_{a_0\eta\pi^0}$	−0.565	1.	
$g_{a_0\eta\pi^0}$	0.584	0.550	1.	$g_{\phi a_0\gamma}$	−0.138	0.657	1.

$$g_{\phi a_0\gamma} = \sqrt{\frac{3}{\alpha}\left(\frac{2M_\phi}{M_\phi^2 - M_{a_0}^2}\right)^3 \Gamma_\phi Br\big(\phi \to \eta\pi^0\gamma\big)}$$
$$= 1.58 \pm 0.10 \pm 0.16\ \mathrm{GeV}^{-1}. \qquad (7)$$

In the NS case $g_{\phi a_0\gamma}$ can be determined directly and is compatible with the value of Eq. (7).

The a_0 width obtained from Eq. (8) is $\Gamma_{a_0}(M_{a_0}) \simeq 105$ MeV. From the NS fit a total decay width $\Gamma_{a_0}(M_{a_0}) \simeq 80$ MeV can be evaluated according to Eq. (10).

In Table 5 the correlation coefficients among the a_0 parameters are shown.

The systematic uncertainties on the parameters account for:

(i) sensitivity to the fixed parameters (the a_0 coupling to $\eta'\pi^0$, $g_{a_0\eta'\pi^0}$, and $g_{\phi K^+K^-}$ in the KL model, M_{a_0} in the NS model);
(ii) normalization uncertainty;
(iii) data–MC discrepancy of the fraction of wrong photon pairings (12% from data and 14% from MC).

5. Unfolding of the $\eta\pi^0$ invariant mass distribution

In order to allow a better comparison with other experimental results and with theoretical models, the invariant mass distribution should be corrected for resolution and smearing effects. Therefore an unfolding procedure has been applied to the $\eta\pi^0$ invariant mass distributions by using the method described in [18]. This is an iterative procedure based on the Bayes theorem, which does not require the inversion of the smearing matrix.

The unfolding has been performed separately on both invariant mass distributions before the background subtraction. The smearing matrices are the same used in the fits described in Section 4.

An initial distribution has to be provided as starting point of the iterative procedure; the unfolded distributions obtained starting from the output of the KL fit or from a flat distribution in $M_{\eta\pi^0}$ differ by less than 3%. This difference has been taken into account in the uncertainty evaluation.

The bin by bin average of the two unfolded distributions is used to calculate the differential branching ratio $(1/\Gamma_\phi)(d\Gamma(\phi \to \eta\pi^0\gamma)/dM_{\eta\pi^0})$ reported in Table 6. The uncertainties are both

Table 6
Differential branching ratio: m is the bin center, the errors are the total uncertainties, and the bin width is 6.35 MeV.

m (MeV)	$(1/\Gamma_\phi)(d\Gamma_{\eta\pi^0\gamma}/dm) \times 10^7$ (MeV^{-1})	m (MeV)	$(1/\Gamma_\phi)(d\Gamma_{\eta\pi^0\gamma}/dm) \times 10^7$ (MeV^{-1})
691.53	0.06 ± 0.07	850.35	2.25 ± 0.13
697.88	0.18 ± 0.10	856.71	2.35 ± 0.14
704.24	0.18 ± 0.12	863.06	2.27 ± 0.13
710.59	0.31 ± 0.13	869.41	2.35 ± 0.13
716.94	0.30 ± 0.08	875.76	2.42 ± 0.16
723.29	0.38 ± 0.11	882.12	2.59 ± 0.16
729.65	0.53 ± 0.17	888.47	2.80 ± 0.14
736.00	0.51 ± 0.13	894.82	2.92 ± 0.19
742.35	0.53 ± 0.05	901.18	3.18 ± 0.20
748.71	0.67 ± 0.07	907.53	3.37 ± 0.17
755.06	0.81 ± 0.07	913.88	3.48 ± 0.17
761.41	0.94 ± 0.10	920.24	3.67 ± 0.17
767.76	0.99 ± 0.11	926.59	3.94 ± 0.17
774.12	0.99 ± 0.08	932.94	4.29 ± 0.25
780.47	1.08 ± 0.09	939.29	4.63 ± 0.25
786.82	1.30 ± 0.10	945.65	4.89 ± 0.21
793.18	1.27 ± 0.13	952.00	5.20 ± 0.22
799.53	1.42 ± 0.28	958.35	5.40 ± 0.28
805.88	1.63 ± 0.28	964.71	5.44 ± 0.33
812.24	1.71 ± 0.14	971.06	5.35 ± 0.22
818.59	1.79 ± 0.16	977.41	4.94 ± 0.21
824.94	1.66 ± 0.18	983.76	4.02 ± 0.19
831.29	1.82 ± 0.15	990.12	2.80 ± 0.27
837.65	1.96 ± 0.12	996.47	1.51 ± 0.32
844.00	2.13 ± 0.13		

from statistics (data and MC) and from systematics. The main contribution to the systematic error is the difference between the two unfolded distributions. The correlation of the contents of nearest neighbour bins of invariant mass is about 50%, for next-nearest neighbour bins is about 20%, and is negligible for bin distance greater than two.

An additional uncertainty of 3% on the absolute scale has to be considered, according to Eq. (5).

To check this procedure, the unfolded distribution has been fit to the KL model, without requiring any smearing matrix. The parameters values are in good agreement with those of Table 4.

6. Conclusions

A high statistics study of the process $\phi \to \eta\pi^0\gamma$ has been performed, by selecting the decay chains corresponding to $\eta \to \gamma\gamma$ and $\eta \to \pi^+\pi^-\pi^0$.

$Br(\phi \to \eta\pi^0\gamma) = (7.01 \pm 0.10 \pm 0.21) \times 10^{-5}$ and $(7.12 \pm 0.13 \pm 0.22) \times 10^{-5}$ respectively have been measured.

A simultaneous fit of the two invariant mass distributions has been performed, which shows that the two samples are consistent with each other.

Both models used in the fits, the ϕ-scalar meson coupling through the kaon loop (KL model) and the direct coupling (NS model), are able to reproduce the experimental $\eta\pi^0$ mass distribution.

From the fit results that $\phi \to \eta\pi^0\gamma$ decay is dominated by $\phi \to a_0(980)\gamma$, since the vector contribution is very small, $Br(e^+e^- \to VP \to \eta\pi^0\gamma) < 10^{-6}$.

The fit allows also the extraction of the $a_0(980)$ mass and its couplings to $\eta\pi^0$, K^+K^-, and to the ϕ meson. The mass agrees at one standard deviation level with the PDG value. The two sets of couplings obtained from the fits agree with each other. Using these couplings, a total decay width of the $a_0(980)$ in the range 80–105 MeV is estimated. The ratio $R_{a_0} = g^2_{a_0K^+K^-}/g^2_{a_0\eta\pi^0} \simeq 0.6$–$0.7$ is obtained; this value agrees with the previous measurements. A large $g_{\phi a_0\gamma}$ has been found (1.6–1.8 GeV^{-1}) suggesting a sizeable strange quark content of the $a_0(980)$.

Acknowledgements

We thank the DAΦNE team for their efforts in maintaining low background running conditions and their collaboration during all data-taking. We want to thank our technical staff: G.F. Fortugno and F. Sborzacchi for their dedicated work to ensure an efficient operation of the KLOE Computing Center; M. Anelli for his continuous support to the gas system and the safety of the detector; A. Balla, M. Gatta, G. Corradi, and G. Papalino for the maintenance of the electronics; M. Santoni, G. Paoluzzi, and R. Rosellini for the general support to the detector; C. Piscitelli for his help during major maintenance periods. This work was supported in part by EURODAPHNE, contract FMRX-CT98-0169; by the German Federal Ministry of Education and Research (BMBF) contract 06-KA-957; by the German Research Foundation (DFG), 'Emmy Noether Programme', contracts DE839/1-4; by INTAS, contracts 96-624, 99-37; and by the EU Integrated Infrastructure Initiative HadronPhysics Project under contract number RII3-CT-2004-506078.

Appendix A. Main formulas of the KL model [11]

The scalar term of Eq. (6) has the form:

$$\frac{d\Gamma_{\text{scal}}}{dm} = \frac{2|g_{\phi K^+K^-}g(m)|^2 p_{\eta\pi^0}(M_\phi^2 - m^2)}{3(4\pi)^2 M_\phi^3}\left|\frac{g_{a_0K^+K^-}g_{a_0\eta\pi^0}}{D_{a_0}(m)}\right|^2$$

where

$$p_{\eta\pi^0} = \frac{\sqrt{[m^2 - (M_\eta - M_{\pi^0})^2][m^2 - (M_\eta + M_{\pi^0})^2]}}{2m}.$$

The detailed formulation of the KL function $g(m)$ can be found in [11]. $D_{a_0}(m)$ is the inverse propagator of the a_0:

$$D_{a_0}(m) = M_{a_0}^2 - m^2 + \sum_{ab}\left[\text{Re}\,\Pi_{ab}(M_{a_0}) - \Pi_{ab}(m)\right].$$

The sum is extended over all the possible two particle decays of the a_0: $ab = \eta\pi^0$, K^+K^-, $K^0\bar{K}^0$, and $\eta'\pi^0$.

The a_0 width is:

$$\Gamma_{a_0}(m) = \frac{\sum_{ab} \mathrm{Im}\, \Pi_{ab}(m)}{m} = \frac{\sum_{ab} g^2_{a_0 ab} \rho_{ab}(m)}{16\pi m} \tag{8}$$

where:

$$\rho_{ab}(m) = \sqrt{\left(1 - \frac{(m_a + m_b)^2}{m^2}\right)\left(1 - \frac{(m_a - m_b)^2}{m^2}\right)}.$$

The parameters of the scalar term that are determined by the fit are the a_0 mass and the couplings $g_{a_0 K^+K^-}$ and $g_{a_0\eta\pi^0}$. The a_0 to $\eta'\pi^0$ coupling is fixed either to $g_{a_0\eta'\pi^0} = -\sqrt{2}\cos\varphi_P\, g_{a_0K^+K^-}$ ($qq\bar{q}\bar{q}$ hypothesis) or to $g_{a_0\eta'\pi^0} = 2\sin\varphi_P\, g_{a_0K^+K^-}$ ($q\bar{q}$ hypothesis), where φ_P is the pseudoscalar mixing angle (the value $\varphi_P = 39.7°$ has been used [19]). Another fixed parameter is the coupling of the ϕ to the K^+K^- pair:

$$g_{\phi K^+K^-} = \frac{M_\phi \sqrt{48\pi Br(\phi \to K^+K^-)\Gamma_\phi}}{(M^2_\phi - 4M^2_K)^{3/4}} = 4.49 \pm 0.07.$$

Appendix B. Main formulas of the NS model [13]

The differential decay width of the NS model is the following:

$$\frac{d\Gamma_{th}(\phi \to \eta\pi^0\gamma)}{dm} = \frac{8\pi\alpha}{3} \frac{p_{\eta\pi^0}(M^2_\phi - m^2)^3}{M^3_\phi} \times \left| \frac{g_{\phi a_0 \gamma}\, g_{a_0\eta\pi^0}}{m^2 - M^2_{a_0} + iM_{a_0}\Gamma_{a_0}(m)} + \frac{\mathrm{b}_0}{M^2_\phi} + \frac{\mathrm{b}_1}{M^4_\phi}\left(m^2 - M^2_{a_0}\right) + A_{\mathrm{vect}} \right|^2. \tag{9}$$

The resonance width is mass dependent according to [14]:

$$\Gamma_{a_0}(m) = \Gamma_{\eta\pi^0}(m) + \Gamma_{K^+K^-}(m) + \Gamma_{K^0\bar{K}^0}(m)$$

where:

$$\Gamma_{\eta\pi^0}(m) = \frac{g^2_{a_0\eta\pi^0}}{8\pi m^2} p_{\eta\pi^0};$$

$$\Gamma_{K\bar{K}}(m) = \frac{g^2_{a_0K^+K^-}}{16\pi m}\sqrt{1 - (2M_K/m)^2} \quad \text{for } m > 2M_K;$$

$$\Gamma_{K\bar{K}}(m) = \frac{ig^2_{a_0K^+K^-}}{16\pi m}\sqrt{(2M_K/m)^2 - 1} \quad \text{for } m < 2M_K \tag{10}$$

(with $K\bar{K} = K^+K^-$, $K^0\bar{K}^0$).

The scalar background is parametrized with a polynomial with two complex coefficients, b_0 and b_1. The vector background, A_{vect}, takes into account all processes $e^+e^- \to V \to V'P_1$ with $V' \to P_2\gamma$ ($V, V' = \rho, \omega, \phi$ and $P_{1,2} = \eta, \pi^0$).

References

[1] E. Klempt, A. Zaitsev, Phys. Rep. 454 (2007) 1;
D.V. Bugg, Phys. Rep. 397 (2004) 257;
C. Amsler, N.A. Törnqvist, Phys. Rep. 389 (2004) 61;
F.E. Close, N.A. Törnqvist, J. Phys. G: Nucl. Part. Phys. 28 (2002) R249.

[2] M.D. Scadron, et al., Phys. Rev. D 69 (2004) 014010.

[3] R.L. Jaffe, Phys. Rev. D 15 (1977) 267;
R.L. Jaffe, Phys. Rep. 409 (2005) 1;
L. Maiani, et al., Phys. Rev. Lett. 93 (2004) 212002;
G. 't Hooft, et al., Phys. Lett. B 662 (2008) 424.

[4] J. Weinstein, N. Isgur, Phys. Rev. Lett. 48 (1982) 659;
J. Weinstein, N. Isgur, Phys. Rev. D 41 (1990) 2236;
Yu.S. Kalashnikova, et al., Eur. Phys. J. A 24 (2005) 437.

[5] KLOE Collaboration, A. Aloisio, et al., Phys. Lett. B 536 (2002) 209.

[6] SND Collaboration, M.N. Achasov, et al., Phys. Lett. B 479 (2000) 53;
CMD-2 Collaboration, R.R. Akhmetshin, et al., Phys. Lett. B 462 (1999) 380.

[7] KLOE Collaboration, F. Ambrosino, et al., Eur. Phys. J. C 49 (2007) 473;
KLOE Collaboration, F. Ambrosino, et al., Phys. Lett. B 634 (2006) 148;
KLOE Collaboration, A. Aloisio, et al., Phys. Lett. B 537 (2002) 21.

[8] KLOE Collaboration, M. Adinolfi, et al., Nucl. Instrum. Methods A 488 (2002) 51;
KLOE Collaboration, M. Adinolfi, et al., Nucl. Instrum. Methods A 482 (2002) 364;
KLOE Collaboration, M. Adinolfi, et al., Nucl. Instrum. Methods A 492 (2002) 134.

[9] KLOE Collaboration, F. Ambrosino, et al., Nucl. Instrum. Methods A 534 (2004) 403.

[10] C. Amsler, et al., Phys. Lett. B 667 (2008) 1.

[11] N.N. Achasov, V.N. Ivanchenko, Nucl. Phys. B 315 (1989) 465;
N.N. Achasov, A.V. Kiselev, Phys. Rev. D 68 (2003) 014006.

[12] N.N. Achasov, V.V. Gubin, Phys. Rev. D 63 (2001) 094007.

[13] G. Isidori, et al., JHEP 0605 (2006) 049.

[14] S.M. Flattè, Phys. Lett. B 63 (1976) 224.

[15] A. Bramon, et al., Phys. Lett. B 283 (1992) 416.

[16] D.V. Bugg, et al., Phys. Rev. D 50 (1994) 4412.

[17] D.V. Bugg, Phys. Rev. D 78 (2008) 074023.

[18] G. D'Agostini, Nucl. Instrum. Methods A 362 (1995) 487.

[19] KLOE Collaboration, F. Ambrosino, et al., Phys. Lett. B 648 (2007) 267.